Crystal Structures from Building Blocks: The Metallates

By Helmut ESCHRIG and Helge ROSNER (Dresden)

Summary

While stacking is the dominating structure argument for undirected binding (ionic, metallic, van der Waals), bond co-ordination is the dominating structure argument for covalent binding. The vast variety of structures of multi-component systems arises because complexes of one type of binding may figure as components in another type of binding. Particularly, extended covalent components (chains, planes, three-dimensional networks) may form the anionic component in an otherwise ionic crystal. Within well defined classes of materials where the structural units are understood, new structures may be anticipated. Extended networks of structural complexes may cause superstructures.

Zusammenfassung

Während Kugelpackung das dominierende Strukturargument für ungerichtete Bindung ist (ionische, metallische, van-der-Waals-Bindung), ist Bindungskoordination das dominierende Strukturargument für kovalente Bindung. Die riesige Vielfalt von Strukturen mehrkomponentiger Systeme entsteht, weil Komplexe eines Bindungstypes die Rolle von Komponenten in einem anderen Bindungstyp spielen können. Insbesondere können ausgedehnte kovalente Komplexe (Ketten, Ebenen, dreidimensionale Netze) die anionischen Komponenten in einem ansonsten ionischen Kristall bilden. Im Rahmen wohldefinierter Materialklassen, in denen die Struktureinheiten wohlverstanden sind, können neue Strukturen antizipiert werden. Ausgedehnte Netze von Stukturkomplexen können Überstrukturen hervorrufen.

1. Introduction

Atoms or molecules stick together in crystals by chemical bonds. Hence, their exists an intimate relation between chemical binding and crystal structures. There are basically four types of chemical binding: ionic binding, metallic binding, van der Waals binding, and covalent binding. If we leave

aside for a moment the case of molecular crystals, then the first three types are essentially undirected while covalent binding is directed by its very nature.

Undirected means that the binding forces are central pair forces, of long range in ionic crystals, and of short range in metallic and van der Waals crystals. In metals, there is additionally to the pair forces an isotropic pressure of the Fermi liquid of conduction electrons. Spatial inhomogeneities of that conduction electron liquid due to electron-ion interaction lead to many-particle forces (BROVMAN and KAGAN 1974, HARRISON 1973) in addition to the central pair force of isotropically screened ions, however the latter force dominates in the hierarchy of interactions leading to a hierarchy of structural arguments.

Undirected binding by central pair forces favours close-packed structures. For one-component crystals they are obtained by stacking close-packed triangular layers of spheres on top of each other. Depending on the stacking order one obtains face-centred cubic or hexagonal crystal structures. The body-centred cubic structure being not far from close-packed may also appear. Multi-component materials crystallize into close packings of spheres of several radii: two types of spheres with rather different radii prefer the NaCl structure, while for nearly equal sphere radii the CsCl structure is preferred. If the stoichiometric ratio is 2:1 instead of 1:1, for certain ratios of radii various Laves phases form (SCHULZE 1974). Dominant structural arguments derived from the principle of close packing are the maximization of space filling by spheres and the maximization of co-ordination numbers.

Molecules are not spherical, and even the pair forces have usually multipole components. Hence stacking of molecules in molecular crystals results in greater variety and lower symmetry.

Covalent binding leads to a completely different situation. What matters here are bond lengths and bond angles. Bond angles are related to at least three-body forces as three centres are needed to define an angle. If the bonds are formed by atomic (sp)-shells, then low co-ordination numbers 4 (as in silicon and diamond) or 3 (as in graphite and polymers) result. Covalent bonds formed by atomic d-shells result again in low co-ordination numbers 2 or 4 in cases of low point symmetry, and in co-ordination numbers 6 or 8 for cubic point symmetry (see Fig. 1.). Orbitals engaged in a covalent bond and having their lobes of density stretched in the direction of the bond are called σ-orbitals. Strong covalent bonds are σ-bonds.

In the materials which we are going to consider in more detail in this paper, covalent complexes extending through the whole crystal are immersed in an ionic surroundings. A well known case is given by the cubic perovskites, as for instance $BaTiO_3$, shown in Fig. 2. An anionic network of covalently

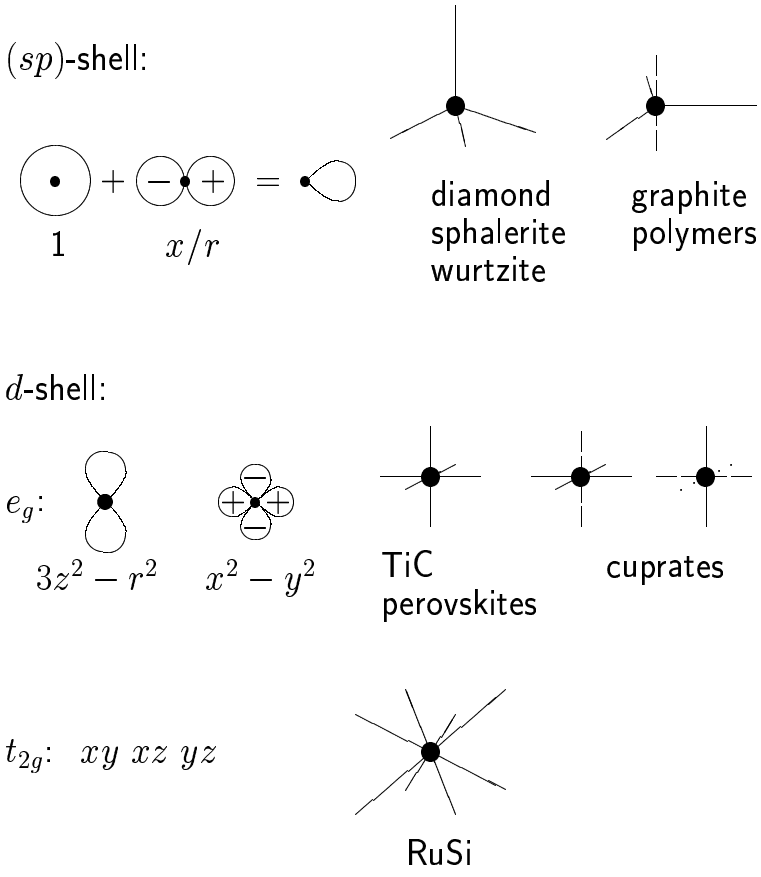

Figure 1: Covalent bonds from (sp)- and d-orbitals: the angular dependence of the orbitals engaged is given on the left, and the bond geometry on the right. The superposition of an s- and a p-orbital gives a directed lobe orbital, resulting in a tetrahedral co-ordination, if all three p-orbitals are engaged, and in a trigonal planar co-ordination, if only two of the tree p-orbitals are engaged, the third one orthogonal to the plane may form the π-bonds of organic chemistry. A single d-orbital engaged leads to a twofold linear or a fourfold planar co-ordination. In a cubic point symmetry, either the e_g group of orbitals is engaged leading to a sixfold octahedral co-ordination, or the t_{2g} group leads to an eightfold cubic co-ordination.

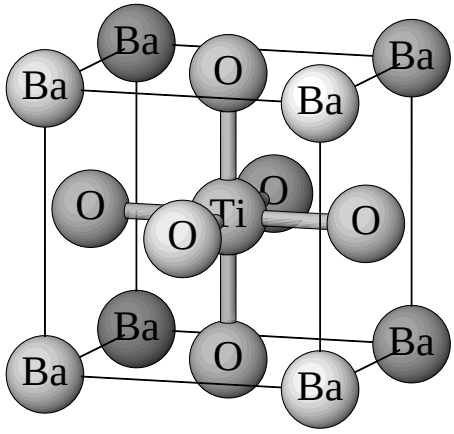

Figure 2: The unit cell of $BaTiO_3$. The rods indicate strong covalent bonds between Ti and O. By periodically repeating this unit cell one obtains an anionic oxygen-edge sharing network of TiO_3 octahedra.

bound oxygen-edge sharing TiO_3 octahedra is immersed in a simple cubic lattice of Ba cations.

One also finds in nature covalently bound complexes immersed in a metallic surroundings. Examples are given by the Zintl phases.

In the following section we recall some relevant features of a covalent bond, which we need for the discussion of the cuprate complexes in Section 3. The cuprates form an already extensively investigated case of the broader class of metallates (titanates, vanadades, manganates, nickelates and so on) with similar structural and binding features, and with a great variety of surprising physical properties. An overview over chain cuprate structures is given in Section 4, and the planar cuprate structures are considered in Section 5. Stripe superstructures in planar cuprates which have become a very topical subject of investigation recently are considered in Section 6.

2. The Covalent Bond

The simplest and for semi-quantitative arguments in most cases sufficiently accurate description of a covalent bond is obtained in the molecular field approximation, where one describes the motion of a valence electron on a single-particle quantum orbital in the average 'molecular' field of the nuclei and all other electrons present.

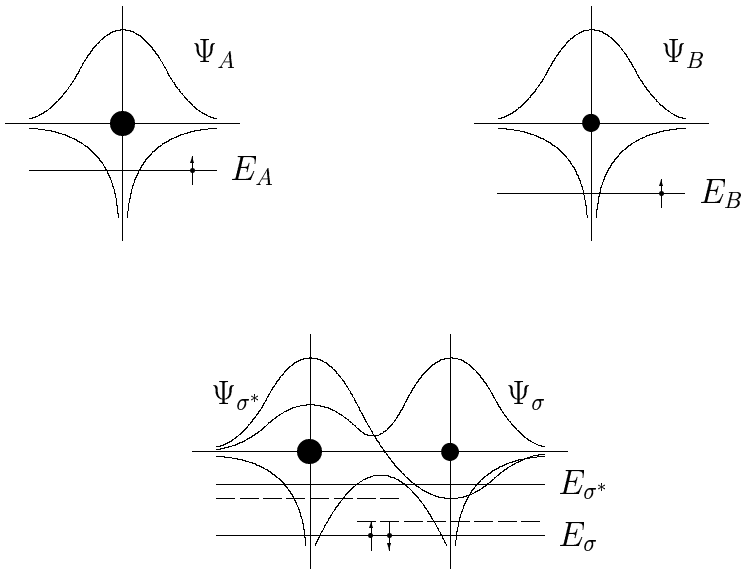

Figure 3: The orbitals, the potentials of the molecular field, and the orbital energy levels of a covalent bond as described in the text. The dots indicate the atomic centres.

Consider two atoms A and B having one valence electron each, which occupies the highest occupied atomic orbital with energy E_A and E_B, respectively. Let Ψ_A and Ψ_B be the orbital wave functions (Fig. 3.). If the atoms are brought close to each other, the atomic orbitals begin to overlap and hybridize into two orthonormal to each other molecular orbitals Ψ_σ and Ψ_{σ^*} with energy levels E_σ and E_{σ^*}. By orthonormality demands, the bonding orbital Ψ_σ has one node less than the anti-bonding orbital Ψ_{σ^*}. The amplitude of the bonding orbital is larger at the atom with the lower atomic orbital energy level (B in the case of Fig. 3.), and E_σ is lower than this lower atomic orbital energy. The amplitude of the antibonding orbital is larger at the atom with the higher atomic orbital energy level, and E_{σ^*} is above this higher atomic orbital energy. (These findings remain valid, if the atoms A and B are of the same species, and $E_A = E_B$. In this case one

still has $E_\sigma < E_{\sigma^*}$ due to the difference in the node number. Of course, the amplitudes on both atoms are now the same.)

Since every molecular orbital may be occupied by two electrons with opposite spin direction, both valence electrons of the former atoms A and B may now occupy the bonding orbital with orbital energy E_σ. The (positively counted) binding energy is then $E_A + E_B - 2E_\sigma$. If the atomic orbitals were already occupied with two electrons each, then the four electrons would have to occupy both the bonding and anti-bonding molecular orbitals, and there were no binding, since $E_A + E_B = E_\sigma + E_{\sigma^*}$. It is easily seen that there is a covalent binding energy gain, provided that one of the molecular orbitals, Ψ_σ or Ψ_{σ^*}, is partially occupied, or the bonding orbital is fully occupied and the anti-bonding orbital is empty, in which case the covalent binding energy is maximum.

These considerations show that there are two main prerequisites of covalency: there must be a resonance of atomic levels (if the energies E_A and E_B were very different, then the amplitude of the molecular orbitals would be negligibly small at one of the atoms, and ionicity would result instead of covalency), *and there must be partial occupation of either the bonding or the anti-bonding molecular orbital, or full occupation of the bonding orbital only.*

3. The cuprate complex

The basic element of all cuprate compounds is the planar CuO_4 plaquette. It is shown in Fig. 4. together with the relevant covalent σ-orbitals. The shell occupation of the Cu^{+2}-ion is $3d^9 4s^0$, and that of the O^{-2}-ion is $2p^6$. (In order to simplify ionicity notations in the sequel, we use the notation Cu^{+2} instead of the commonly used notation Cu^{2+}.) The nominal anionic redox number of this complex is -6: $[CuO_4]^{-6}$. The highest occupied atomic orbitals are copper $3d$-orbitals and oxygen $2p$-orbitals. Most of those orbitals are non-bonding. There is one σ-orbital at each ion with the angular dependencies of the wavefunction given by $(x^2 - y^2)/r^2$ for the Cu $3d$-orbital and by x/r and y/r, respectively, for the O $2p$-orbitals. (The plane of the plaquette was taken to be the $x - y$-plane of a Cartesian co-ordinate system.)

The relevant molecular orbital energy level scheme is sketched in Fig. 4. The strong covalent $dp\sigma$ bond leads to an energy splitting between the bonding and anti-bonding levels as large as 10eV. The fully occupied non-bonding Cu $3d$ and O $2p$ levels are in between. Since due to the ionic $3d^9$ and $2p^6$ occupations one electron is missing compared to full $3d$ and $2p$ shells, the anti-bonding $dp\sigma^*$-level must be half-filled. Hence, the prerequisites for covalency are fulfilled. (The energy distance between the Cu $3d$-level and the oxygen

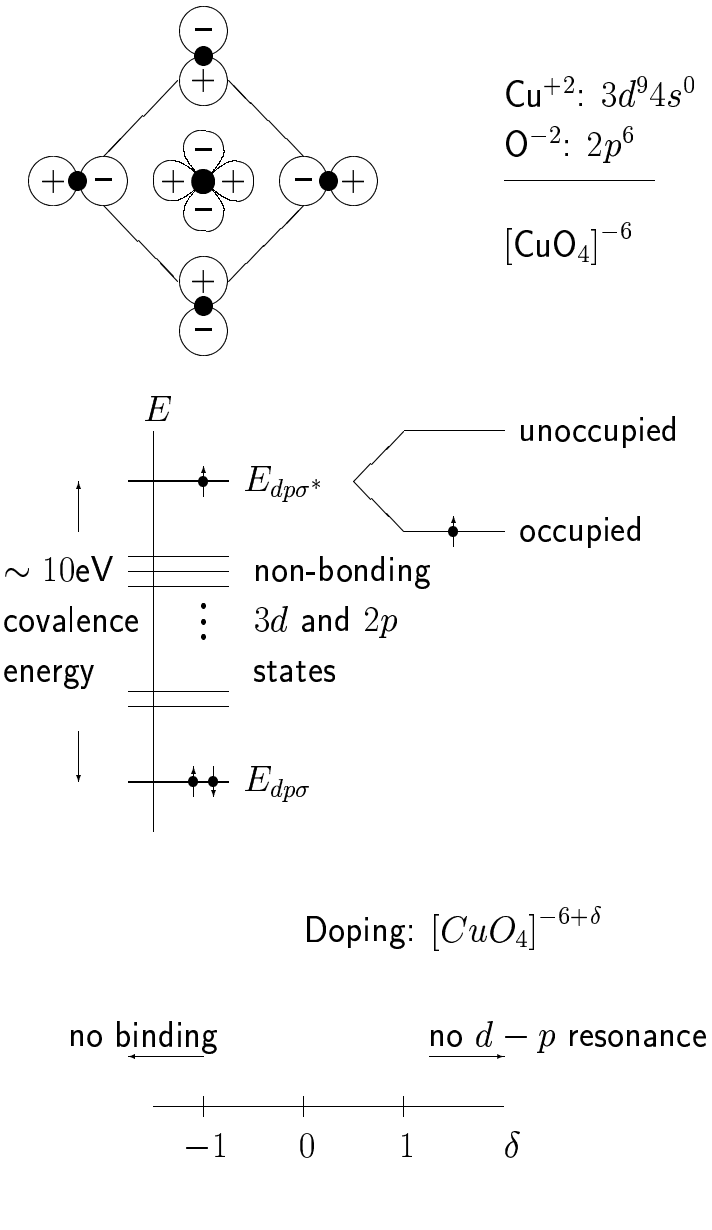

Figure 4: The covalent CuO_4-plaquette, relevant for the cuprates. The copper ion resides in the centre of the plaquette, and the four oxygen ions occupy the corners. The anti-bonding molecular orbital is shown with sign changes of the wavefunction on all four Cu-O-bonds, so that the wavefunction has nodes on the bonds like Ψ_{σ^*} in Fig. 3. See the text for further explanations.

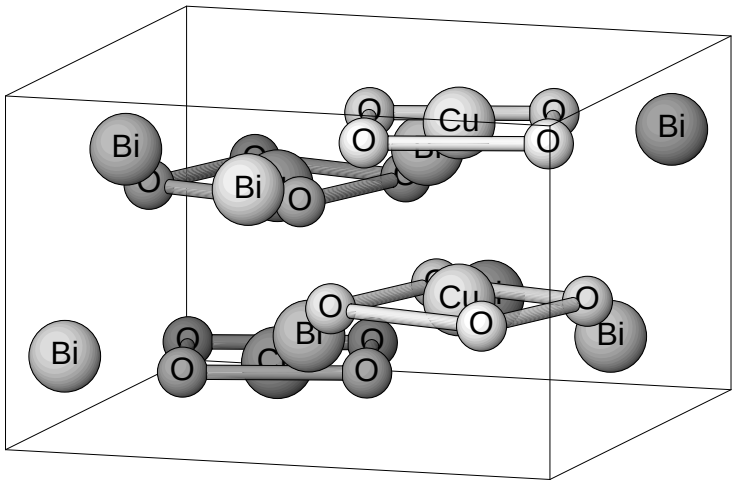

Figure 5: Unit cell of the Bi_2CuO_4 crystal. Here and in the sequel the rods are used to make the planar CuO_4-plaquette stand out. The strong covalent σ-bonds are between the central copper and the four surrounding oxygens.

$2p$-level in the molecular field is roughly 3eV and hence small compared to the covalency splitting.) Due to a strong intra-atomic correlation of the Cu $3d$-orbitals, the molecular field approximation is, however, not sufficient here to describe the electronic properties, and the half-filled anti-bonding level splits due to these correlations into a lower and an upper 'Hubbard' level, each accessible to one electron only. The lower Hubbard level is occupied.

In the sequel, doping of the CuO_4-plaquette will be an important issue. The doping charge is named δ in Fig. 4. If the plaquette is doped with electrons ($\delta < 0$), then the anti-bonding level gets filled and covalency gets reduced. At $\delta = -1$, the anti-bonding band is full, and there cannot be any covalent $dp\sigma$-binding any more. Doping the plaquette with holes ($\delta > 0$) increases covalency. However, at large doping rates the oxygen potential is moved down against the copper potential (while copper remains essentially $3d^9$), and the level resonance gets reduced, which reduces covalency again. Hence, *the CuO_4-plaquette is strongly covalently bound around half-filling of the anti-bonding $dp\sigma^*$-orbital.*

4. Chain cuprate structures

The idea to build up planar cuprate structures by linking CuO_4-plaqettes which share in one or two oxygen ions is due to MÜLLER-BUSCHBAUM (1977).

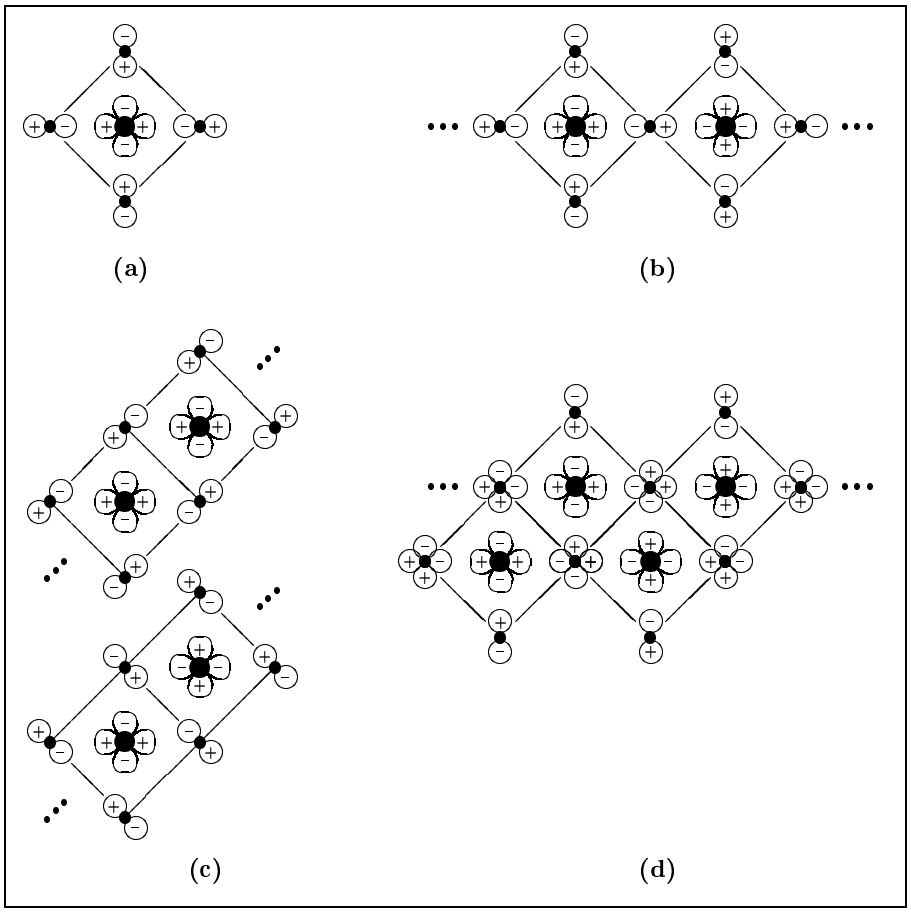

Figure 6: Cuprate chains formed from the plaquette (a) as the building block. A corner-sharing chain (b), an edge-sharing chain (c), and a double-chain (d) are shown. See text for further explanations.

He made a systematic study of the cuprate structures long before the high-T_c superconductors were discovered.

The isolated CuO_4-plaquette has the very high reduction state -6, and the only structure known where it appears is Bi_2CuO_4 (Müller-Buschbaum 1977, García-Muñoz et al. 1990). The unit cell of this crystal structure is shown in Fig. 5.

In order to have the same covalency situation with a lower reduction state, CuO_4-plaquettes may share in oxygen ions. A number of possibilities is sketched in Fig. 6. If a row of plaquettes is formed where adjacent plaquettes share in a corner, a one-dimensional periodic anionic $[CuO_3]^{-4}$-complex results as shown in Fig. 6(b). As seen from this figure, subsequent

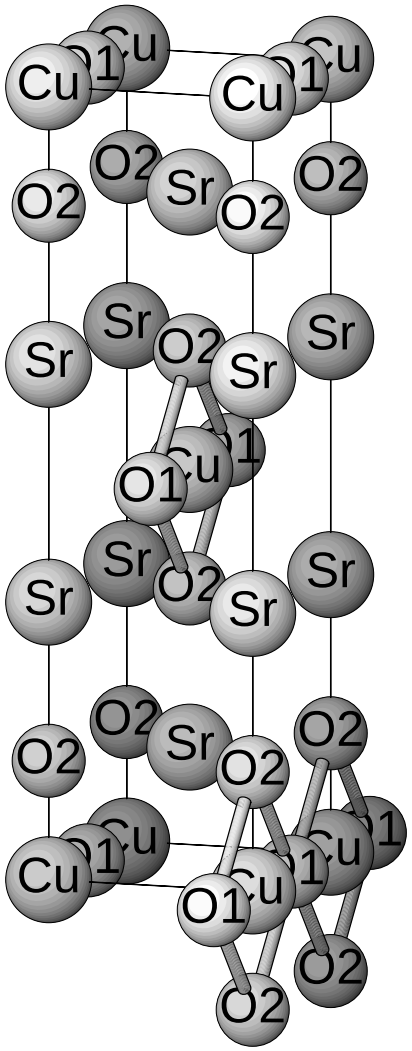

Figure 7: Unit cell of Sr_2CuO_3. The cuprate chains run along the direction perpendicular to the drawing plane. There is a regular array of projections of those chains on the drawing plane.

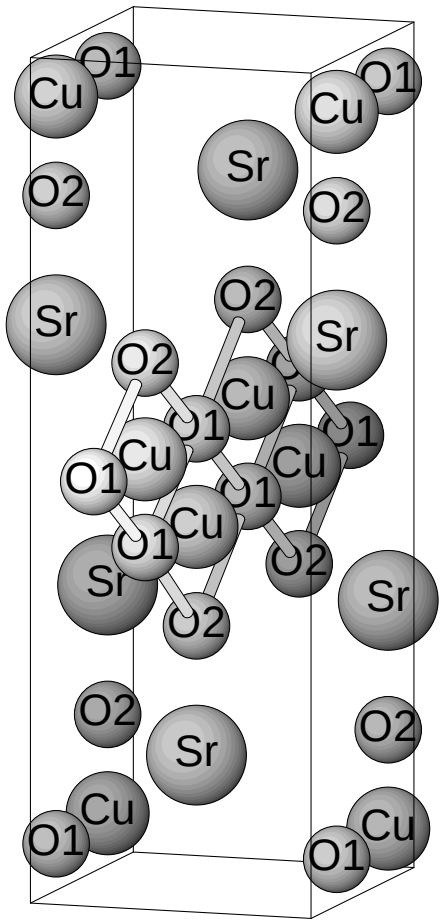

Figure 8: Unit cell of $SrCuO_2$. The double-chains are arranged like the chains in Fig. 7.

orbitals along the chain have a relative phase factor -1 in the totally anti-bonding state. That means that the one-dimensional energy band of this chain in molecular field approximation has its maximum at the Brillouin zone boundary. If one forces subsequent orbitals to have the same phase

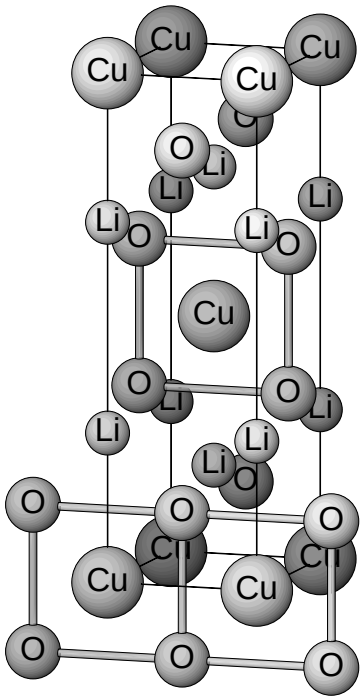

Figure 9: Unit cell of Li_2CuO_2. The edge-sharing chains run left-right in the drawing plane.

for a zero wave vector of the Bloch state, then the state cannot be fully anti-bonding any more: the band has its minimum at the centre (Γ-point) of the Brillouin zone. Without any calculation one finds a cosine-like anti-bonding band with its minimum at the zone centre and its maximum at the zone boundary. Close to half-filling this band is again correlation split into a lower and an upper Hubbard sub-band, and the material is a semiconductor instead of a one-dimensional metal. Examples of this case are Sr_2CuO_3 and Ca_2CuO_3 (Teske and Müller-Buschbaum 1969). They became very recently highly topical materials because of their magnetic properties as prototypes of nearly one-dimensional Heisenberg chains (see e.g. Rosner et al. (1997) and citations therein). The unit cell of Sr_2CuO_3 is shown in Fig. 7.

Fig. 6(c) shows two different anti-bonding states on an edge-sharing chain of cuprate plaquettes. This chain is formed by anionic $[CuO_2]^{-2}$-complexes with a further reduced reduction state. With the phase rules as described above the upper pattern belongs to a zone-centre state, and the lower pattern belongs to a zone-boundary state. Both are maximally anti-bonding, but are not quite σ-states. They are different in energy due to the crystal-field split

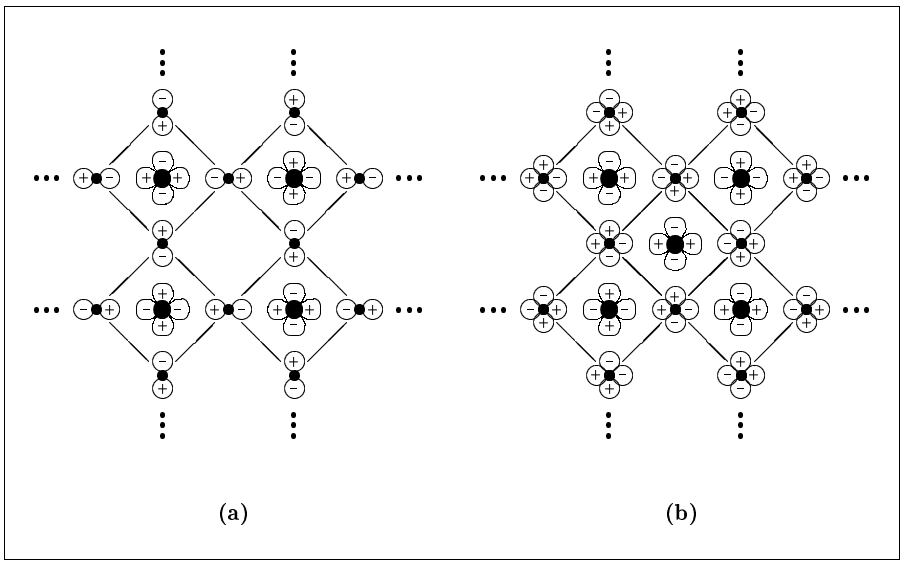

Figure 10: Cuprate planes formed from plaquettes as the building block. The checkerboard pattern (a) may be obtained by joining together chains of Fig. 6(b). The pattern (b) is obtained by putting an additional copper ion on every other white field in horizontal rows of the checkerboard (a).

between the two different oxygen $2p$-orbitals engaged. This type of chains is found in Li_2CuO_2 (Hoppe und Rieck 1970) and in $CuGeO_3$ (Hidaka et al. 1997), which latter is to be understood as $(GeO)CuO_2$ in our context. This material causes much interest at present due to a possible spin-density wave groundstate.

The same reduction state $[CuO_2]^{-2}$ is realized in the double-chain of Fig. 6(d), which is present in $SrCuO_2$ (Matsushita et al. 1994). This material (see Fig. 8) is magnetically even more one-dimensional then Sr_2CuO_3. A whole family of multileg ladder compounds $Sr_{2n}Cu_{2n+2}O_{4n+2}$ seems to exist (Ishida et al. 1996) and is presently celebrated because of the interesting magnetic properties.

5. Plane cuprate structures

By joining together periodically repeated CuO_3-chains of Fig. 6(b) so that adjacent chains share in the side oxygen ions of those chains, the checkerboard-like planar structure of Fig. 10(a) is obtained. This is an anionic $[CuO_2]^{-2}$-plane for nominal valence charges. Doping with holes yields the famous $[CuO_2]^{-2+\delta}$-plane of the high-T_c superconductors (see Pickett (1989) for

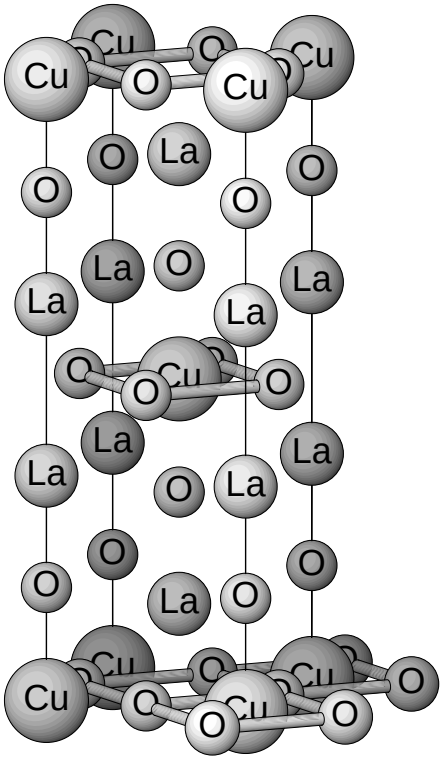

Figure 11: Unit cell of La_2CuO_4.

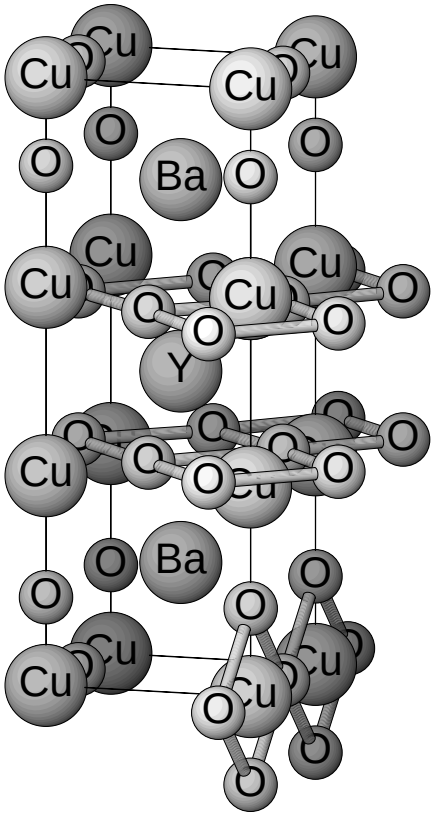

Figure 12: Unit cell of $YBa_2Cu_3O_7$.

an overview). The undoped plane ($\delta = 0$) is isolating with an antiferromagnetic groundstate. Already at low doping rates it becomes a strange metal, and for $\delta \gtrapprox 0.1$ (as well as for electron doping $\delta \lessapprox -0.1$) it becomes superconducting.

The material for which high-T_c superconductivity was first discovered was barium doped La_2CuO_4, which in our context is to be understood as $(LaO)_2CuO_2$. Its structure is shown in Fig. 11. It consists of a stacking of two ionic $[LaO]^+$-planes followed by a covalent $[CuO_2]^{2-}$-plane, on top of each other. If La is partially replaced by Ba (or Sr), hole-doping results in the CuO_2-plane. For the understanding of that material it is crucial that the oxygen of the BaO-plane (the so-called apical oxygen because it forms the apex of an oxygen pyramid whose basis is the CuO_4-plaquette) is at most very weakly covalently bound to the CuO_2-plane.

The high-T_c material investigated in most detail is $YBa_2Cu_3O_7$, which for our context is $YBa_2(CuO_2)_2(CuO_3)$. Its structure is shown in Fig. 12. It

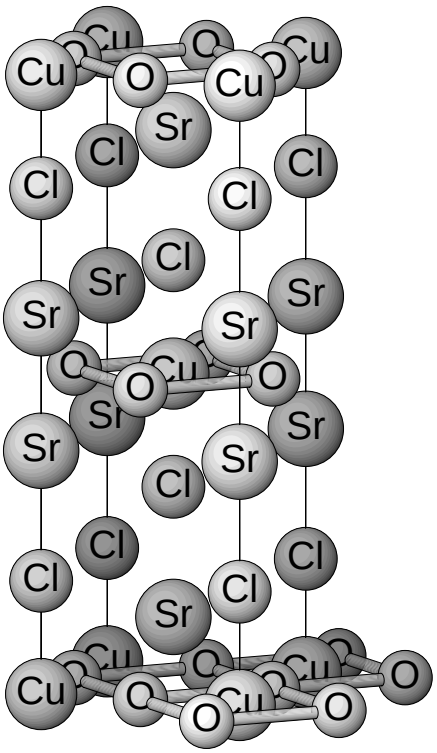

Figure 13: Unit cell of $Sr_2CuO_2Cl_2$.

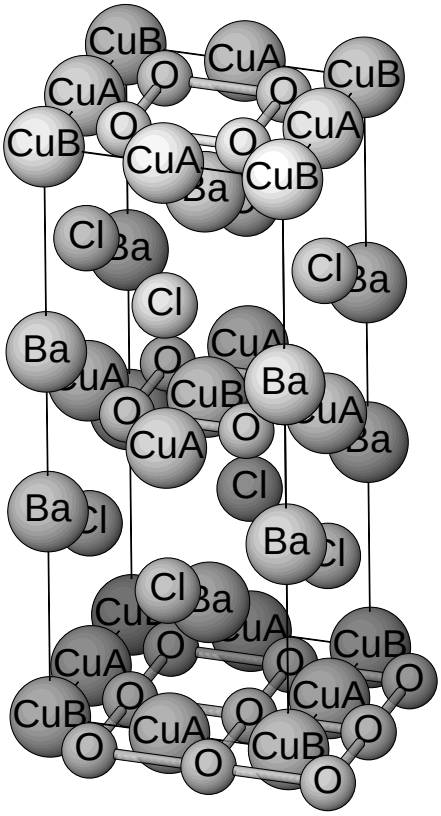

Figure 14: Unit cell of $Ba_2Cu_3O_4Cl_2$.

contains both CuO_2-planes and CuO_3-chains immersed in a lattice of barium and yttrium ions. By counting charges one finds that compared to nominal charges of those covalent cuprate structures one hole must be shared by two planes and one chain. Hence, the planes are $[CuO_2]^{-2+\delta}$ and the chains are $[CuO_3]^{-3-2\delta}$.

Recently another planar cuprate, $Sr_2CuO_2Cl_2$, became famous because it cleaves easily in the Cl-plane, and allowed for the first time precise photoemmission measurements of the excitation spectra of an *undoped* CuO_2-plane (Wells et al.). Its structure is shown on Fig. 13.

Finally, an even less reduced anionic plane of $[Cu_3O_4]^{-2}$ is obtained by periodically repeating the pattern of Fig. 10(b). Here, the anionic charge -2 relates to three copper ions instead of one. It is obtained, if one places additional copper on every other white field in the rows of the checkerboard pattern of Fig. 10(a). Other than the original ones the new Cu ions do not form cuprate chains: their plaquette wavefunctions engage oxygen p-orbitals

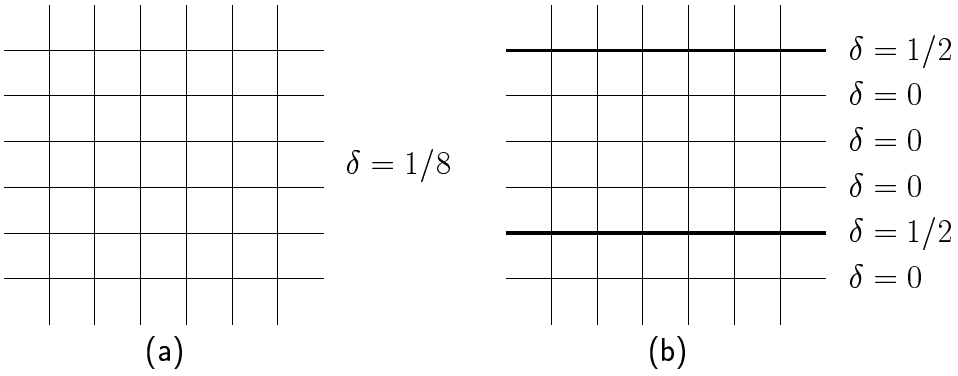

Figure 15: Stripes obtained by doping charge disproportionation on the cuprate plane as explained in the text.

which are not shared by adjacent plaquettes. Hence those states only weakly hybridize into a very narrow band. This plane is realized in $Ba_2Cu_3O_4Cl_2$. The structure is shown in Fig. 14. (see PITSCHKE et al. (1995)). The two different plaquettes of this cuprate plane lead to two very different electronic excitation spectra (GOLDEN et al. 1997), and among other things to two subsequent magnetic order transitions into antiferromagnetism.

6. Stripes

Very recently, more and more experimental evidence (BIANCONI 1994, TRANQUADA 1996) of a stripe superstructure, at least dynamically, in the $[CuO_2]^{-2+\delta}$-planes has been found. Superconductivity occurs roughly for $0.1 \lessapprox \delta \lessapprox 0.2$. On the other hand, for $\delta = 0.5$ the lower Hubbard subband of the correlated anti-bonding states would be half-filled, a situation which would give rise to a Peierls instability in one dimensional structures. Electron-lattice interaction would lead to a cusp-like minimum of the total energy as a function of the band filling at half-filling.

One could think now of a scenario (DRECHSLER et al. 1997), where the charge disproportionates on the cuprate plane in a way shown in Fig. 15. The holes, originally homogeneously distributed over the cuprate plane, may coalesce into rows, thus forming a one-dimensional structural element, and adjust to a doping rate of $\delta = 0.5$ in those rows, whereas the rows inbetween are undoped. For an average doping $\delta = 1/6$, which is the optimum value for superconductivity, one would obtain every third row doped. The undoped double-chain inbetween would have antiferromagnetic correlations with a spin

gap, which is considered to favour superconductivity.

Fig. 15 shows the situation with an average doping rate $\delta = 1/8$ which leads to every fourth row charged. The triple-chain inbetween has no spin gap. One could speculate that the obscure breakdown of superconductivity in a very narrow range of δ around 1/8 might be connected with a pinning of this situation into a static superstructure.

Bibliography

Bianconi, A.: On the Possibility of new High T_c Superconductors by producing Metal Heterostructures as in the Cuprate Perkowskites. Solid State Commun. *89*, 933–936 (1994)

Brovman, E. G. and Kagan, Yu. M.: Phonons in Non-Transition Metals. In: Horton, G. K. and maraduduin, A. A. (Eds.): Dynamical properties of Solids, vol. I, p. 191–300. Amsterdam: North-Holland 1974

Drechsler, S.-L., Málek, J., Eschrig, H., Rosner, H., and Hayn, R.: Electronic Structure and BOW-CDW States of CuO_3 Chains. J. Supercond. *10*, 393–396 (1997)

García-Muñoz, J. L., Rodríguez-Carrajal, J., Sapiña, F., Sanchis, M. J., Ibáñez, R., and Beltrán-Porter, D.: Crystal and magnetic structures of Bi_2CuO_4. J. Phys. Condens. Matter *2*, 2205–2214 (1990)

Golden, M. S., Schmelz, H. C., Knupfer, M., Haffner, S., Krabbes, G., Fink, J., Yushankhay, V., Rosner, H., Hayn, R., Müller, A., and Reichardt, G.: Dispersion of a Hole in a Two-Dimensional Cu_3O_4 Plane: A Tale of Two Singlets. Phys. Rev. Lett. *78*, 4107–4110 (1997)

Harrison, W. A.: Multi-ion interactions and structures in simple metals. Phys. Rev. *B7*, 2408–2416 (1973)

Hidaka, M., Hatae, M., Yamada, I., Nishi, M., and Akimitsu, J.: Reexamination of the room temperature crystal structure of $CuGeO_3$ by x-ray diffraction experiments: observation of new superlattice reflections. J. Phys.: Condens. Matter *9*, 809–824 (1997)

Hoppe, R. und Rieck, H.: Die Kristallstruktur von Li_2CuO_2. Z. anorg. allg. Chem. *379*, 157–164 (1970)

Ishida, K., Kitaoka, Y., Tokunga, Y., Matsumoto, S., Asayama, K., Azuma, M., Hiroi, Z., and Takano, M.: Spin correlation and spin gap in quasi-one-dimensional spin-1/2 cuprate oxides: A ^{63}Cu NMR study. Phys. Rev. *B53*, 2827–2834 (1996)

Matsushita, Y., Oyama, Y., Hasegawa, M., and Takei, H.: Growth and Structural Refinement of Orthorhombic $SrCuO_2$ Crystals. J. Solid State Chem. *114*, 289–293 (1994)

Müller-Buschbaum, H.: Oxometallate mit ebener Koordination. Angew. Chem. *89*, 704–717 (1977)

Pickett, W. E.: Electronic structure of the high-temperature oxide superconductors. Rev. Mod. Phys. *61*, 433–512 (1989)

Pitschke, W., Krabbes, G., and Mattern, N.: Powder diffraction data and Rietveld refinement of the compound $Ba_2Cl_2Cu_3O_4$. Powder Diff. *10*, 282–287 (1995)

Rosner, H., Eschrig, H., Hayn, R., Drechsler, S.-L., and Málek, J.: Electronic structure and magnetic properties of the linear chain cuprates Sr_2CuO_3 and Ca_2CuO_3. Phys. Rev. *B56*, 3402–3412 (1997)

Schulze, G. E. R.: Metallphysik. p. 83ff. Wien: Springer 1974

Teske, C. L. and Müller-Buschbaum,H.: Zur Kenntnis von Sr_2CuO_3. Z. Anorg. Allg. Chem. *371*, 325–332 (1969)

Tranquada, J. M.: Stripe correlations of spins and holes in cuprates and nickelates. Ferroelectrics *177*, 43–57 (1996)

Wells, B. O., Shen, Z.-X., Matsuura, A., King, D. M., Kastner, M. A., Greven, M., and Birgenau, R. J.: E versus $\boldsymbol{k}$ Relations and Many-Body Effects in the Model Insulating Copper Oxide $\mathbf{Sr_2CuO_2Cl_2}$. Phys. Rev. Lett. *74*, 964–967 (1995)